Infrared Study of *n*-Alkanes in CCl_4, $CDCl_3/CCl_4$, and $CDCl_3$ 0.5% Solutions

R. A. NYQUIST* and S. L. FIEDLER

Analytical Sciences Laboratory, 1897F Building, Dow Chemical Company, Midland, Michigan 48667

Three factors appear to affect *n*-alkane molecular vibrations in $CHCl_3/CCl_4$ solutions. These are: (1) Physical restriction of the νCH_3 and νCH_2 vibrations by solvent molecules. (2) Intermolecular hydrogen bonding between *n*-alkane protons and the free pair of electrons on Cl atoms of either CCl_4 or $CDCl_3$. The positively charged alkane protons arise during the dipole moment changes, $\delta P/\delta Q$, occurring during a full cycle of the νCH_3 and νCH_2 modes. (3) The physical restriction of solvent molecules, which is greater in the case of $CDCl_3$ than in the case of CCl_4 due to a high degree of $CDCl_3$ orientation about *n*-alkane molecules due to repulsion of the C-D of $CDCl_3$ by the *n*-alkane νCH_3 and νCH_2 protons, which allows stronger C-D:Cl bonds to be formed between solute and solvent.

Index Headings: **Infrared; Solvent effects; Intermolecular hydrogen bonding.**

INTRODUCTION

Many vibrational studies of alkanes have been reported over the years, and these studies have recently been summarized by Lin-Vien *et al.*[1] and by Colthup *et al.*[2] We have studied a variety of chemical compounds in dilute solutions using IR spectroscopy in an attempt to gain an understanding of solute–solvent interactions.[3-36] The present study of *n*-alkanes in dilute solution in CCl_4, 54.6 mole % $CDCl_3/CCl_4$, and $CDCl_3$ solution is an extension of our interest in solute–solvent interactions. These studies have aided us in the elucidation and identification of molecular structure using IR spectroscopy as an analytical tool.

EXPERIMENTAL

Infrared data were recorded with a Nicolet 710 FT-IR system. Samples of the *n*-alkanes were prepared as 0.5% wt/volume in CCl_4, and in $CDCl_3$. One milliliter of the stock solution for each *n*-alkane in CCl_4 solution was mixed with 1 mL of the same *n*-alkane in $CDCl_3$ solution. These solutions were placed separately in a 0.5-mm sealed KBr cell, and the IR spectra for each *n*-alkane in three different solvent systems were recorded. The temperature in the laboratory is kept at 71 ± 1°F. Therefore, the sample temperature is also at 71 ± 1°F, and the sample is not heated in the FT-IR instrument during the short time the sample solutions are in the instrument compartment.

RESULTS AND DISCUSSION

Frequency Data for νCH_3 and νCH_2 Vibrations. The *n*-alkanes have the empirical structure CH_3-$(CH_2)_n$-CH_3 and can be represented by the formula C_nH_{2n+2} (where *n* is the number of carbon atoms in any member of the series).

Table I lists the IR data for asymmetric CH_3 stretching ($\nu_{asym}CH_3$) and symmetric CH_3 stretching ($\nu_{sym}CH_3$) for *n*-alkanes at 0.5 wt/vol % with the use of CCl_4, 54.6 mole % $CDCl_3/CCl_4$, and $CDCl_3$ as the solvent system. The $\nu_{asym}CH_3$ mode for each *n*-alkane *increases* in frequency, progressing in the solvent system CCl_4, 54.6 mole % $CDCl_3/CCl_4$, and $CDCl_3$, while the $\nu_{sym}CH_3$ mode *decreases* in frequency, progressing in the solvent system CCl_4, 54.6 mole % $CDCl_3/CCl_4$, and $CDCl_3$. The shift of $\nu_{asym}CH_3$ to higher frequency in going from CCl_4 solution to 54.6 mole % $CDCl_3/CCl_4$ solution varies between 0.02 and 0.08 cm^{-1}, and the shift to higher frequency for $\nu_{asym}CH_3$ varies between 0.11 and 0.22 cm^{-1} in going from CCl_4 solution to $CDCl_3$ solution (see Table II). Generally this shift of $\nu_{asym}CH_3$ to lower frequency becomes larger as the number of carbon atoms in the *n*-alkanes increases. The shift to lower frequency for $\nu_{sym}CH_3$ varies between 0.2 and 0.52 cm^{-1} in going from CCl_4 solution to 54.6 mole % $CDCl_3/CCl_4$, and $CDCl_3$, and the shift to lower frequency for $\nu_{sym}CH_3$ varies between 0.45 and 0.85 cm^{-1} in going from CCl_4 solution to $CDCl_3$ solution. Generally, this shift of $\nu_{sym}CH_3$ to lower frequency becomes larger as the number of carbon atoms in the *n*-alkanes series increases.

Figure 1 shows a plot of $\nu_{asym}CH_3$ vs. the molecular weight (M.W.) of each *n*-alkane in each of the solvent systems used. The plots for the series pentane-hexane-heptane are linear for each of the solvent systems, and the plots for octane through octadecane are linear for each of the solvent systems. The difference between the slopes of the separate sections of the plots we attribute to the presence of adjacent CH_2 groups. Beginning with octane and higher members of the *n*-alkane series, the addition of more CH_2 groups in the *n*-alkane chain has no additional effect upon $\nu_{asym}CH_3$ in the sequence CH_3-$(CH_2)_{6-16}$-CH_3.

Figure 2 shows plots of $\nu_{sym}CH_3$ vs. the M.W. for each of the *n*-alkanes in each of the three solvents systems. These three plots show that $\nu_{sym}CH_3$ *decreases* in frequency as the M.W. of the *n*-alkane *increases* and that the effect of the $(CH_2)_n$ chain upon the $\nu_{sym}CH_3$ mode is essentially optimized when *n* is 8 or more.

Table III lists IR data for the asymmetric CH_2 stretching mode ($\nu_{asym}CH_2$) and the symmetric CH_2 stretching mode ($\nu_{sym}CH_2$) for each *n*-alkane in each of the three solutions. These data show that the $\nu_{asym}CH_2$ mode *increases* in frequency, progressing in the solvent series CCl_4, 54.6 mole % $CDCl_3/CCl_4$, and $CDCl_3$, while the $\nu_{sym}CH_2$ mode *decreases* in the solvent series CCl_4, 54.6

Received 5 April 1993.

* Author to whom correspondence should be sent.

0003-7028/93/4710-1670$2.00/0

TABLE I. Infrared data for $\nu_{asym}CH_3$ and $\nu_{sym}CH_3$ for *n*-alkanes in 0.5% solutions in CCl_4, 54.6 mole % $CDCl_3/CCl_4$, and $CDCl_3$.

	$\nu_{asym}CH_3$			$\nu_{sym}CH_3$		
Compound	CCl_4 (cm^{-1})	54.6 Mole % $CDCl_3/CCl_4$ (cm^{-1})	$CDCl_3$ (cm^{-1})	CCl_4 (cm^{-1})	54.6 Mole % $CDCl_3/CCl_4$ (cm^{-1})	$CDCl_3$ (cm^{-1})
Pentane	2959.55	2959.57	2959.66	2873.12	2872.92	2872.67
Hexane	2958.69	2958.74	2958.80	2872.92	2872.67	2872.34
Hexane	2959.23	2959.26	2959.31	2873.05	2872.81	2872.54
Heptane	2958.86	2958.91	2958.98	2872.81	2872.54	2872.23
Octane	2958.62	2958.66	2958.73	2872.82	2872.53	2872.20
Nonane	2958.46	2958.50	2958.58	2872.79	2872.50	2872.17
Decane	2958.35	2958.41	2958.49	2872.78	2872.49	2872.14
Undecane	2958.14	2958.22	2958.33	2872.70	2872.42	2872.05
Dodecane	2958.03	2958.09	2958.23	2872.66	2872.33	2871.96
Tridecane	2957.94	2958.02	2958.10	2872.65	2872.31	2871.91
Tetradecane	2957.79	2957.85	2957.99	2872.60	2872.24	2871.81
Octadecane	2957.26	2957.34	2957.48	2872.35	2871.83	2871.50
Δ cm^{-1}	−2.29	−2.23	−2.18	−0.77	−1.09	−1.17

mole % $CDCl_3/CCl_4$, and $CDCl_3$. Table IV compares the frequency shifts for $\nu_{asym}CH_2$ and $\nu_{sym}CH_2$ for each of the *n*-alkanes in going from solution in CCl_4 to solution in 54.6 mole % $CDCl_3/CCl_4$, and in going from solution in CCl_4 to solution in $CDCl_3$. The $\nu_{asym}CH_2$ mode frequency increase for *n*-alkanes varies between 0.12 and 0.22 cm^{-1} in going from solution in CCl_4 to solution in 54.6 mole % $CDCl_3/CCl_4$, and the frequency increase varies between 0.23 and 0.41 cm^{-1} in going from solution in CCl_4 to solution in $CDCl_3$. The $\nu_{sym}CH_2$ mode frequency decrease for the *n*-alkanes varies from between 0.01 and 0.41 in going from solution in CCl_4 to solution in 54.6 mole % $CDCl_3/CCl_4$ and between 0.06 and 0.61 in going from solution in CCl_4 to solution in $CDCl_3$.

Figure 3 shows plots of $\nu_{asym}CH_2$ for *n*-alkanes vs. the M.W. of the *n*-alkane for each of the three different dilute solvents. Significant differences are noted for the plot segments hexane through nonane and decane through octadecane.

Figure 4 shows a plot of $\nu_{sym}CH_2$ for the *n*-alkanes in all three solvent systems vs. the M.W. of the *n*-alkane. Again, differences are noted for the plot segments hexane through nonane and decane through octadecane.

Figure 5 shows plots of $\nu_{asym}CH_2$ vs. $\nu_{sym}CH_2$ for the *n*-alkanes in each of the solvent systems.

Again, significant differences are noted for the plot segments hexane through nonane and decane through octadecane.

Figure 6 shows plots of $\nu_{asym}CH_3$ vs. $\nu_{sym}CH_3$ for *n*-alkanes in all three solvents. These plots indicate that the effect of the CH_2 groups upon the νCH_3 frequencies is relatively constant when the value of *n* is 5 or more for $CH_3\text{-}(CH_2)_n\text{-}CH_3$.

Figure 7 shows plots of $\nu_{sym}CH_3$ vs. $\nu_{sym}CH_2$ for *n*-alkanes in all three solvent systems. Linear relationships are apparent for the series heptane through nonane and decane through tridecane with only a slight change in the slope between the plot of tetradecane and octadecane.

An explanation is needed for the behavior of $\nu_{asym}CH_3$, $\nu_{sym}CH_3$, $\nu_{asym}CH_2$, and $\nu_{sym}CH_2$ for *n*-alkanes with change in the solvent system. As discussed previously, both $\nu_{asym}CH_3$ and $\nu_{asym}CH_2$ increased in frequency while $\nu_{asym}CH_3$ and $\nu_{asym}CH_2$ decreased in frequency, progressing in the solvent systems CCl_4, 54.6 mole % $CDCl_3/CCl_4$, $CDCl_3$. During a cycle of $\nu_{asym}CH_3$, two of the CH_3 protons expand and one contracts during one half of the cycle, while two of the CH_3 protons contract and one expands during the other half of the cycle. During a cycle of $\nu_{sym}CH_3$, the three protons expand during one half of the cycle and the three protons contract during the second half of the cycle. During expansion of two or three C-H bonds, the dipole moment change results from a change to a negative electrical charge on the carbon atom and a positive charge on the proton as the C-H bonds expand. A positive charge on the C-H proton would repulse, say, the D atom of $CDCl_3$ and the C-H proton would hydrogen bond to the free pair of electrons on a Cl atom of $CDCl_3$. During half of the $\nu_{asym}CH_3$ cycle only two protons expand and one protron contracts vs. three protons expanding during half of the $\nu_{sym}CH_3$ cycle. In the other half of the $\nu_{asym}CH_3$ cycle, one protron expands while two protons contract vs. three protons contracting during the other half of the $\nu_{sym}CH_3$ cycle. Thus, the CH_3 protons are less positively charged in the $\nu_{asym}CH_3$ mode than during the $\nu_{sym}CH_3$ mode.

There are two factors which apparently affect the $\nu_{asym}CH_3$ and the $\nu_{sym}CH_3$ frequencies for *n*-alkanes when in solution with CCl_4 and or $CDCl_3$. One factor is the

TABLE II. Infrared data for $\nu_{asym}CH_3$ and $\nu_{sym}CH_3$ for *n*-alkanes in CCl_4, 54.6 mole % $CDCl_3/CCl_4$, and $CDCl_3$ solutions.

	$\nu_{asym}CH_3$		$\nu_{sym}CH_3$	
Compound	CCl_4 minus 54.6 mole % $CDCl_3/CCl_4$ (cm^{-1})	CCl_4 minus $CDCl_3$ (cm^{-1})	CCl_4 minus 54.6 mole % $CDCl_3/CCl_4$ (cm^{-1})	CCl_4 minus $CDCl_3$ (cm^{-1})
Pentane	0.02	0.11	−0.20	−0.45
Hexane	0.03	0.08	−0.24	−0.51
Heptane	0.05	0.12	−0.27	−0.58
Octane	0.04	0.11	−0.29	−0.62
Nonane	0.04	0.12	−0.29	−0.62
Decane	0.06	0.14	−0.29	−0.64
Undecane	0.08	0.19	−0.28	−0.65
Dodecane	0.06	0.20	−0.33	−0.70
Tridecane	0.08	0.16	−0.34	−0.74
Tetradecane	0.06	0.20	−0.36	−0.79
Octadecane	0.08	0.22	−0.52	−0.85

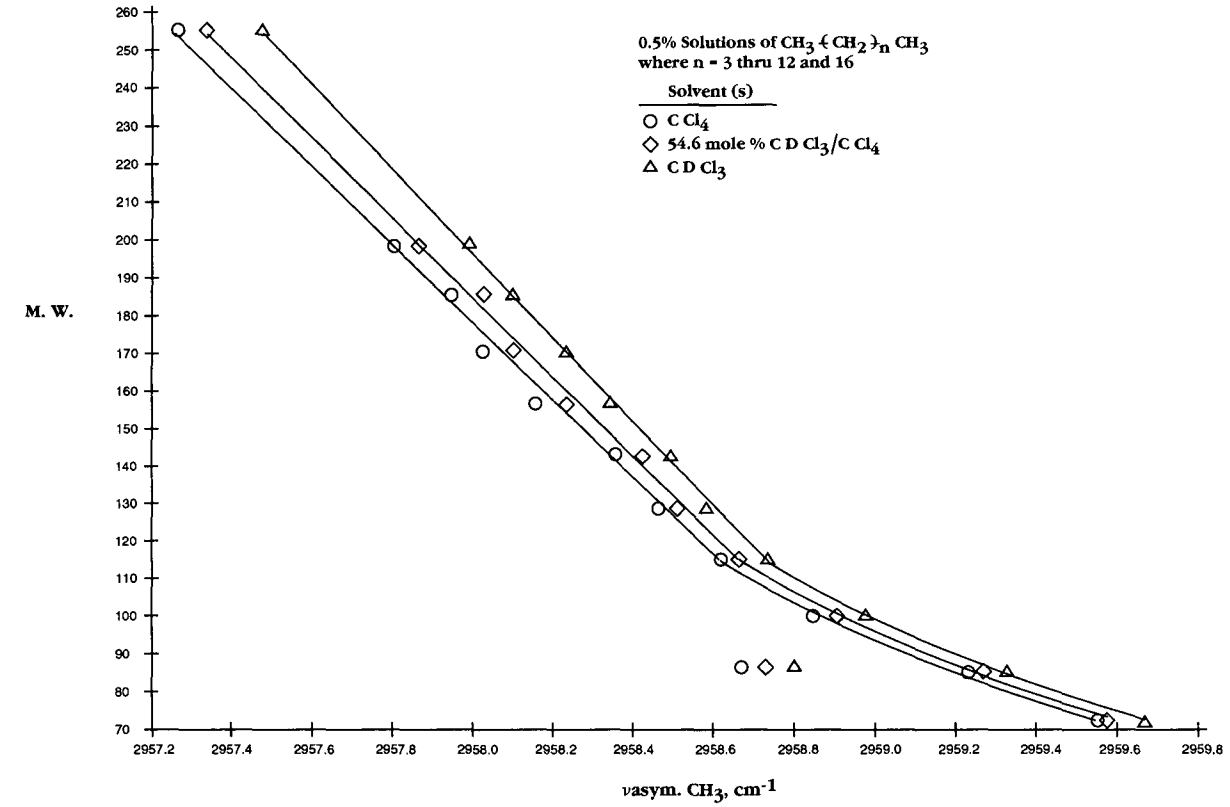

FIG. 1. Plots of $\nu_{asym}CH_3$ (cm^{-1}) vs. the M.W. of each n-alkane in three different solvent systems. The open circle, open diamond, and open triangle points that are at lower frequency and are not connected to the linear plots are for n-hexane of ~95% purity.

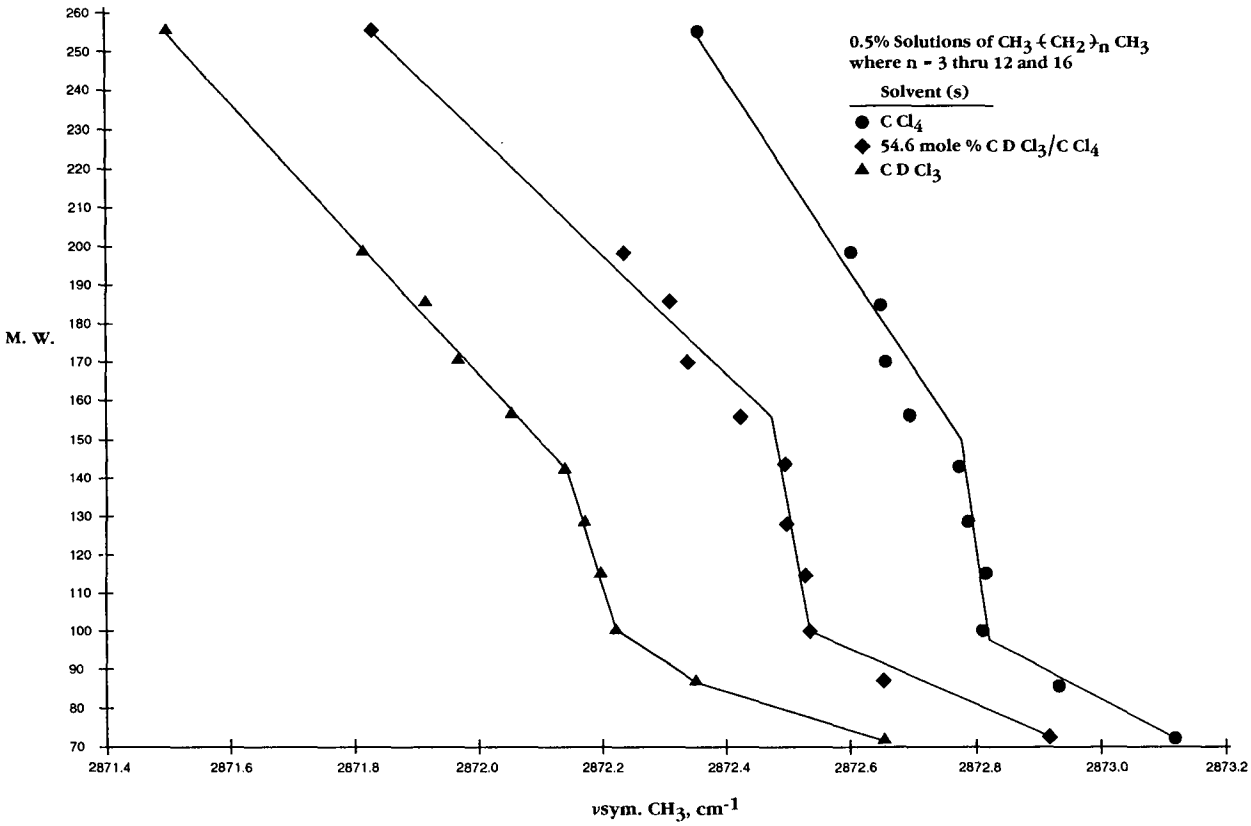

FIG. 2. Plots of $\nu_{sym}CH_3$ (cm^{-1}) vs. the M.W. of each n-alkane in three different solvent systems. The closed circle, closed diamond, and closed triangle that are at lower frequency and are not connected to the plots are for n-hexane of ~95% purity.

Table III. Infrared data for $\nu_{asym}CH_2$ and $\nu_{sym}CH_2$ for *n*-alkanes in 0.5% solutions in CCl_4, 54.6 mole % $CDCl_3/CCl_4$, and $CDCl_3$.

Compound	$\nu_{asym}CH_2$			$\nu_{sym}CH_2$		
	CCl_4 (cm^{-1})	54.6 mole % $CDCl_3/CCl_4$ (cm^{-1})	$CDCl_3$ (cm^{-1})	CCl_4 (cm^{-1})	54.6 mole % $CDCl_3/CCl_4$ (cm^{-1})	$CDCl_3$ (cm^{-1})
Pentane	2927.73	2927.95	2928.14	2861.82	2861.41	2861.21
Hexane	2928.00	2928.16	2928.25	2859.40	2859.32	2859.14
Hexane	2927.89	2928.04	2928.12	2859.12	2858.95	2858.74
Heptane	2927.29	2927.45	2927.58	2857.81	2857.56	2857.37
Octane	2926.95	2927.11	2927.26	2856.55	2856.34	2856.22
Nonane	2926.79	2926.95	2927.07	2855.68	2855.59	2855.58
Decane	2926.83	2926.95	2927.13	2855.31	2855.27	2855.25
Undecane	2926.76	2926.93	2927.03	2855.09	2855.07	2855.05
Dodecane	2926.72	2926.86	2927.01	2854.92	2854.90	2854.88
Tridecane	2926.70	2926.83	2926.98	2854.83	2854.82	2854.79
Tetradecane	2926.66	2926.80	2926.96	2854.77	2854.74	2854.71
Octadecane	2926.61	2926.73	2926.92	2854.59	2854.58	2854.55
Δ cm^{-1}	−1.12	−1.22	−1.22	−7.23	−6.83	−6.66

energy required for the two CH_3 protons of *n*-alkanes to expand against the surrounding solvent molecules. The other factor is hydrogen bonding of the CH_3 protons (charged during the molecular vibration) and the Cl atoms of either CCl_4 or $CDCl_3$. The Cl atoms of CCl_4 are relatively more basic than Cl atoms of $CDCl_3$, and one would expect that intermolecular hydrogen bonding between CH_3 protons and the Cl atoms of CCl_4 would be stronger than with the Cl atoms of $CDCl_3$. Hydrogen bonding is expected to lower the frequency of ν C-H modes, while physical restraint of the $\nu_{asym}CH_3$ and $\nu_{sym}CH_3$ vibrations is expected to raise the frequencies of these vibrations. The largest physical restraint is expected for $\nu_{sym}CH_3$ in CCl_4 and/or $CDCl_3$ solution, since all three protons are expanding in-phase against the solvent molecules. However, the $\nu_{sym}CH_3$ mode for *n*-alkane actually decreases in frequency in going from solution in CCl_4 to solution in $CDCl_3$. This shift to lower frequency is opposite of what is expected in going from solution in CCl_4 to solution in $CDCl_3$, since one would expect a stronger intermolecular hydrogen bond to be formed with the free pair of electrons on the Cl atoms of CCl_4 than for Cl atoms of $CDCl_3$ due to the fact that the Cl atoms are more basic for CCl_4 than for $CDCl_3$. Another factor then must account for this solvent effect. We suggest that there is a difference in the solute–solvent steric factor between *n*-alkane molecules and CCl_4 molecules and *n*-alkane molecules and $CDCl_3$ molecules which allows the CH_3 protons to be spatially nearer $CDCl_3$ Cl atoms than CCl_4 Cl atoms. A shorter bond distance between CH_3 protons and $CDCl_3$ Cl atoms (C-H:Cl) allows a stronger intermolecular hydrogen bond to be formed than in the case of CCl_4 even though the Cl atoms are less basic for $CDCl_3$ than for CCl_4. This point will be discussed more after further discussion of the $\nu_{asym}CH_2$ and $\nu_{sym}CH_2$ vibrations.

As discussed above, the $\nu_{asym}CH_2$ vibration for *n*-alkanes *increases* in frequency, while the $\nu_{sym}CH_2$ vibration *decreases* in frequency in going from CCl_4 solution to $CDCl_3$ solution. This solvent shift behavior for *n*-alkanes is analogous to that exhibited by $\nu_{asym}CH_3$ and $\nu_{sym}CH_3$ in going from solution in CCl_4 to solution in $CDCl_3$, and the same arguments discussed above for the two CH_3 groups apply to the three or more CH_2 groups present in the *n*-alkanes included in this study. Presumably then the CH_2 groups for the *n*-alkanes form the strongest intermolecular hydrogen bonds between $CDCl_3$ Cl atoms rather than CCl_4 Cl atoms, due to a smaller solute–solvent steric factor in the case of $CDCl_3$ compared to CCl_4. If the *n*-alkane exists in a planar zig-zag configuration in solution and the deuteron atom of $CDCl_3$ is repulsed by *n*-alkane protons, then all the $CDCl_3$ Cl atoms would be intermolecularly hydrogen bonded with protons of the CH_3 and CH_2 groups on *n*-alkanes. Thus, the *n*-alkanes would be surrounded by Cl atoms of $CDCl_3$, forming intermolecular hydrogen bonds during νCH_3 and νCH_2 vibrations, and then the C-D groups would be pointing away from the *n*-alkane and forming intermolecular hydrogen bonds with other $CDCl_3$ molecules. This oriented alignment of $CDCl_3$ molecules around the *n*-alkanes existing in a planar zig-zag structure allows a stronger hydrogen bond to be formed between more of the C-H bonds in the case of *n*-alkanes in $CDCl_3$ solutions than in the case of *n*-alkanes in CCl_4 solutions. We suggest that the reason the $\nu_{asym}CH_3$ and $\nu_{asym}CH_2$ modes for *n*-alkanes shift to higher frequency in going from CCl_4 solution to solution in $CDCl_3$ is that only one or two protons

TABLE IV. Infrared data for $\nu_{asym}CH_2$ and $\nu_{sym}CH_2$ for *n*-alkanes in 0.5% solutions in CCl_4, 54.6 mole % $CDCl_3/CCl_4$, and $CDCl_3$.

Compound	$\nu_{asym}CH_2$		$\nu_{sym}CH_2$	
	CCl_4 minus 54.6 mole % $CDCl_3/CCl_4$ (cm^{-1})	CCl_4 minus $CDCl_3$ (cm^{-1})	CCl_4 minus 54.6 mole % $CDCl_3/CCl_4$ (cm^{-1})	CCl_4 minus $CDCl_3$ (cm^{-1})
Pentane	0.22	0.41	−0.41	−0.61
Hexane	0.16	0.25	−0.08	−0.26
Hexane	0.15	0.23	−0.17	−0.38
Heptane	0.16	0.29	−0.25	−0.44
Octane	0.16	0.31	−0.21	−0.33
Nonane	0.16	0.28	−0.09	−0.10
Decane	0.12	0.30	−0.04	−0.06
Undecane	0.17	0.27	−0.02	−0.04
Dodecane	0.14	0.29	−0.02	−0.04
Tridecane	0.13	0.28	−0.01	−0.04
Tetradecane	0.14	0.30	−0.03	−0.06
Octadecane	0.12	0.31	−0.01	−0.06
Δ cm^{-1}	0.10	−0.10	−0.40	−0.55

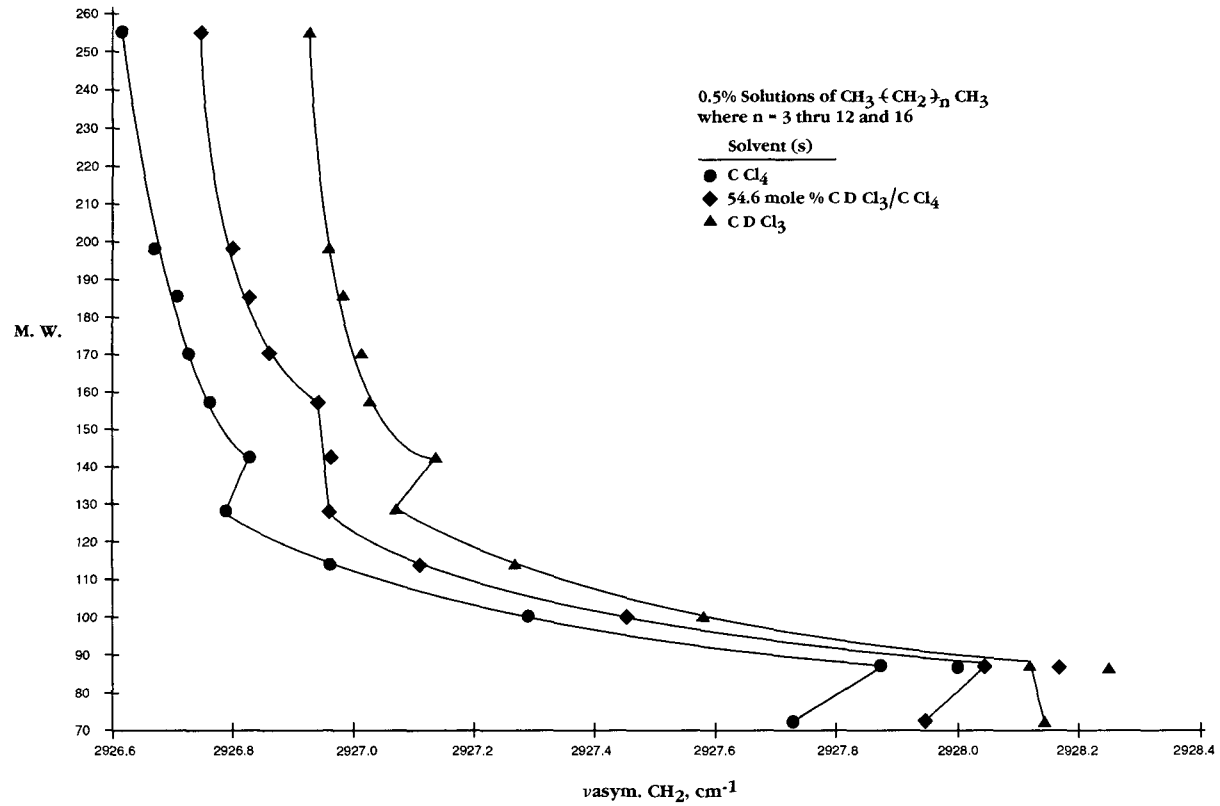

FIG. 3. Plots of $\nu_{asym}CH_2$ (cm^{-1}) vs. the M.W. of each *n*-alkane in three different solvent systems. The closed circle, closed diamond, and closed triangle data points that are at lower frequency and are not connected to the plots are for *n*-hexane of ~95% purity.

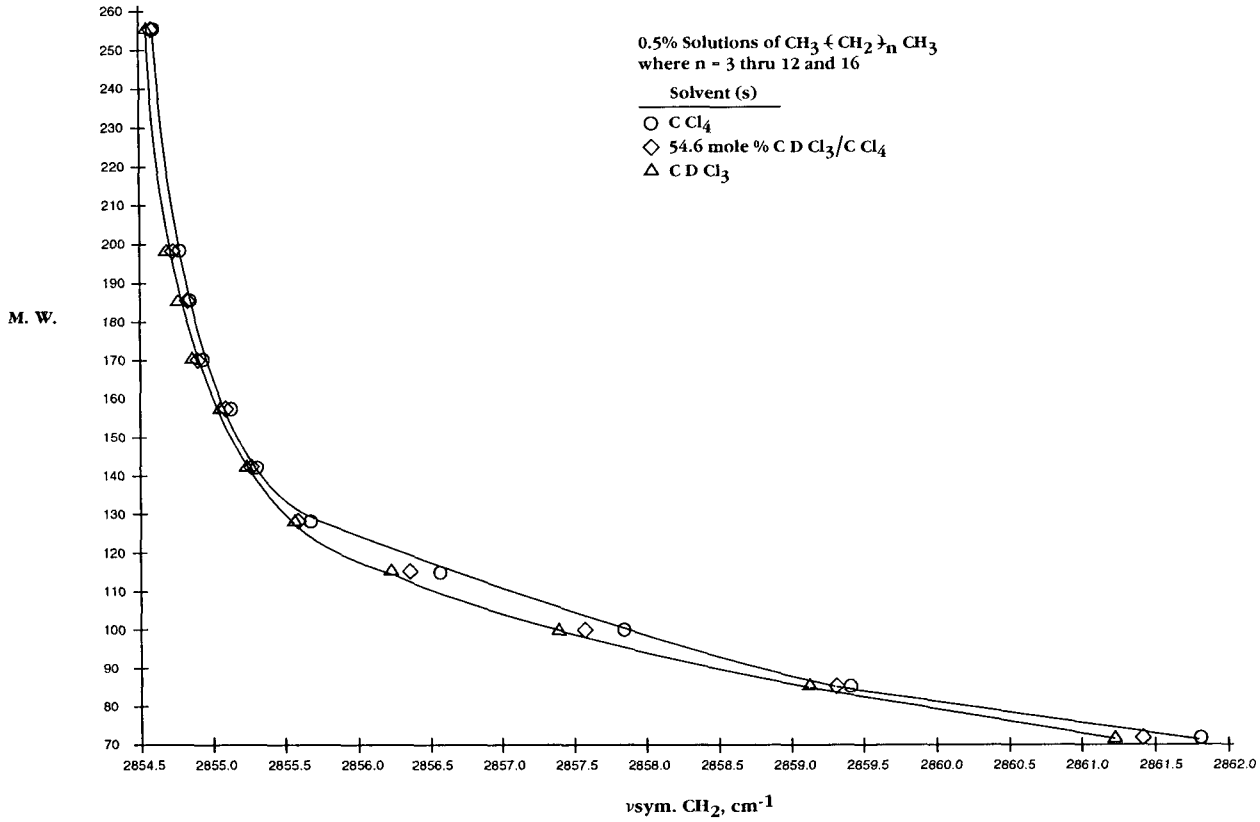

FIG. 4. Plots of $\nu_{sym}CH_2$ vs. the M.W. of each *n*-alkane in three different solvent systems. The open circle, open diamond, and open triangle that are at higher frequency and are not connected with the correct plots are for *n*-hexane of ~95% purity.

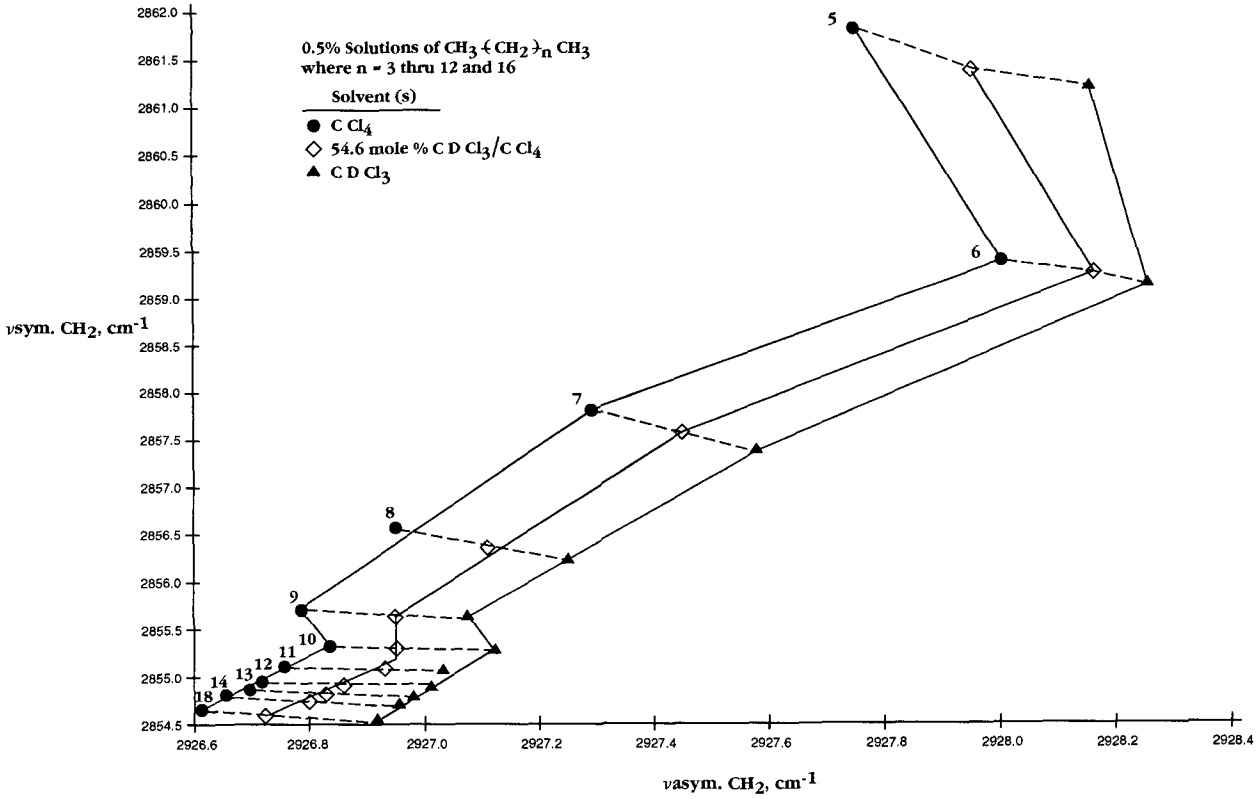

FIG. 5. Plots of $\nu_{asym}CH_2$ vs. $\nu_{sym}CH_2$ for each n-alkane in three different solvent systems.

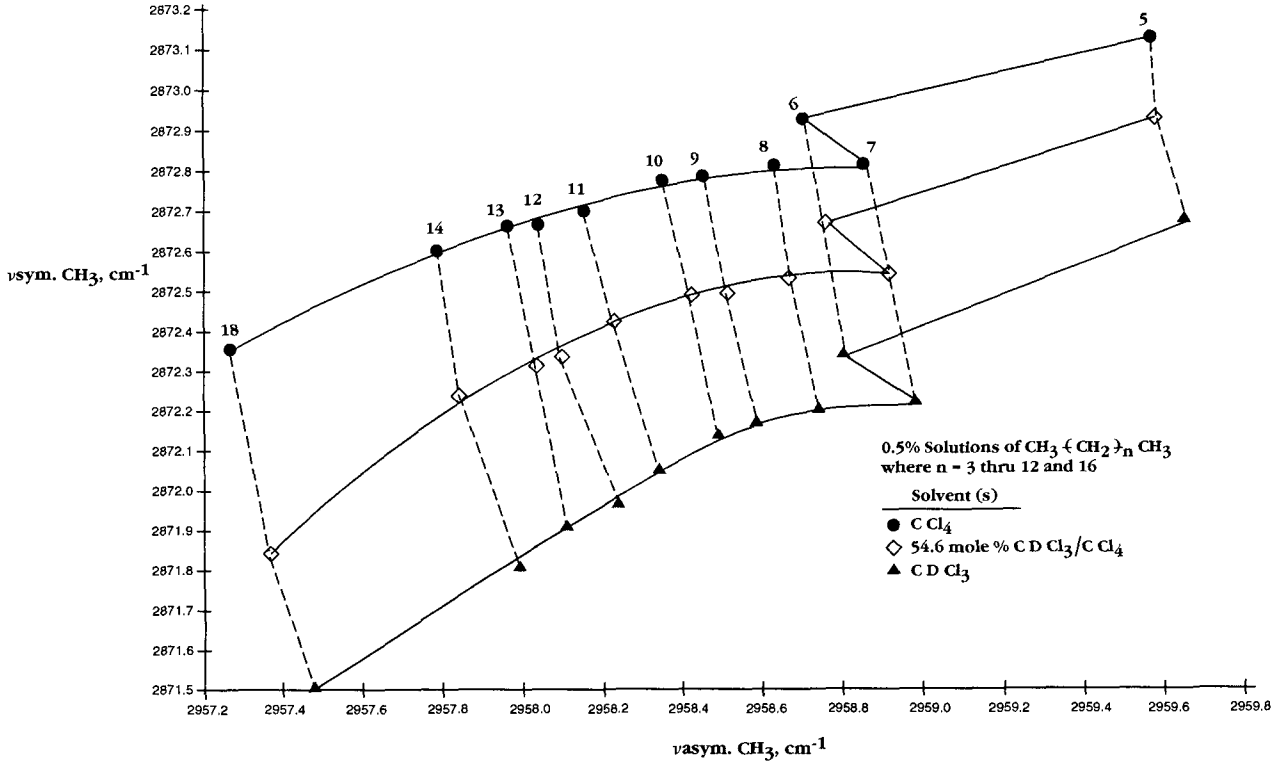

FIG. 6. Plots of $\nu_{asym}CH_3$ vs. $\nu_{sym}CH_3$ for each n-alkane in three different solvent systems.

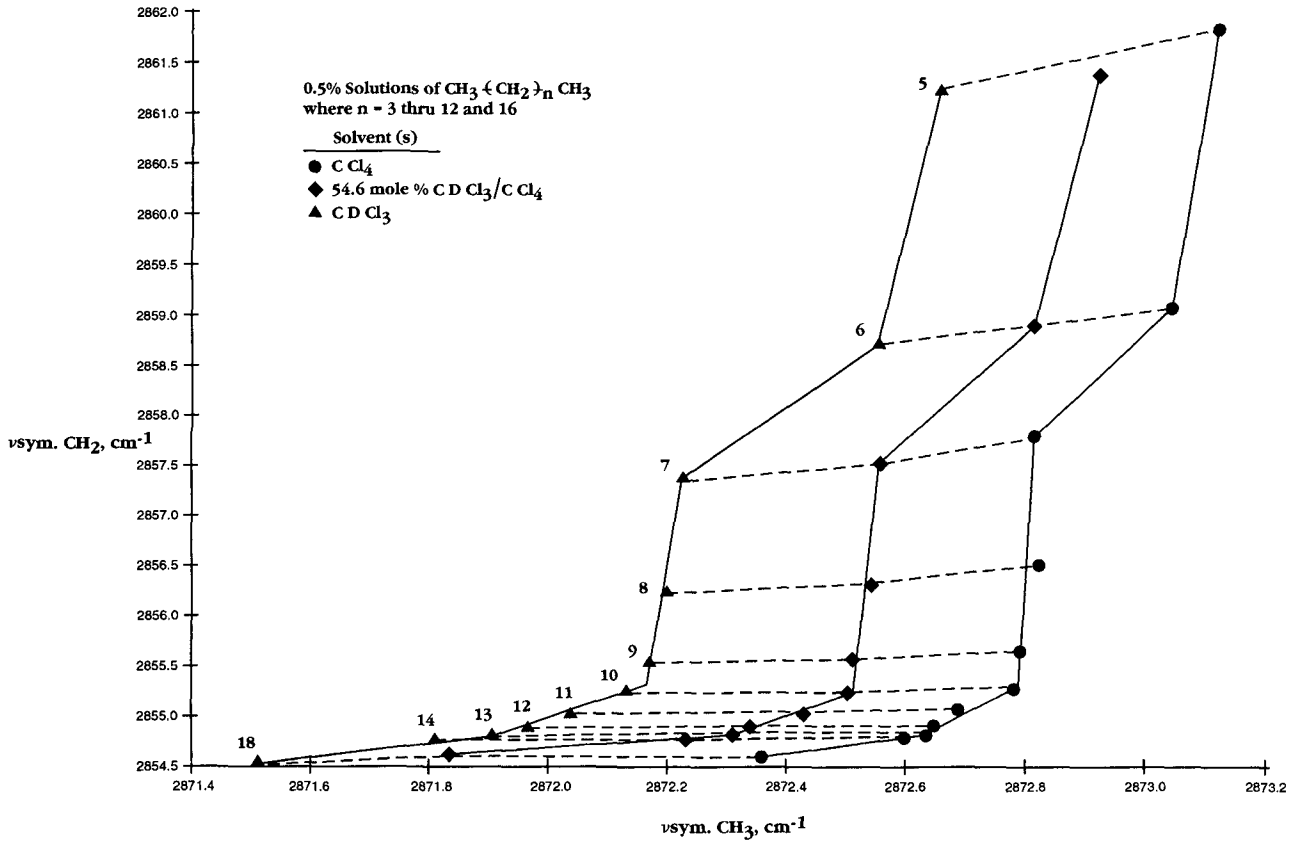

FIG. 7. Plots of $\nu_{sym}CH_3$ vs. $\nu_{sym}CH_2$ for each *n*-alkane in three different solvent systems.

for the CH_3 groups or only one proton for the CH_2 group is forming intermolecular hydrogen bonds with the Cl atoms of CCl_4 or $CDCl_3$ vs. three for the CH_3 group. This factor decreases the effect of hydrogen bonding in lowering νCH frequencies. The energy required to expand the alkane protons against the ordered $CDCl_3$ solvent molecules vs. a lesser order in the CCl_4 solution must more than offset the intermolecular hydrogen bonding effect, since the $\nu_{asym}CH_3$ and $\nu_{asym}CH_2$ modes *n*-alkanes increase in frequency in going from solution in CCl_4 to solution in $CDCl_3$.

Table V lists the frequency separation between $\nu_{asym}CH_3$ and $\nu_{sym}CH_3$ for each of the *n*-alkanes in each of the solvent systems, and Table VI lists the frequency separation between $\nu_{asym}CH_2$ and $\nu_{sym}CH_2$ for each of the *n*-alkanes in each of the solvent systems.

Figure 8 shows plots of the frequency separation between $\nu_{asym}CH_3$ and $\nu_{sym}CH_3$ for *n*-alkanes in all three solvent systems. These plots show that this frequency separation *decreases* as the M.W. or number of carbon atoms in the *n*-alkanes series *increases*.

Figure 9 shows plots of the frequency separation between $\nu_{asym}CH_2$ and $\nu_{sym}CH_2$ for *n*-alkanes in all three solvent systems. These plots show that the frequency separation *increases* as the M.W. or number of carbon atoms in the *n*-alkanes series *increases*. As the number

TABLE V. Infrared data for $\nu_{asym}CH_3$ and $\nu_{sym}CH_3$ for *n*-alkanes in 0.5% solutions in CCl_4, 54.6 mole % $CDCl_3/CCl_4$, and $CDCl_3$.

	$\nu_{asym}CH_3$, $\nu_{sym}CH_3$		
Compound	CCl_4 (cm^{-1})	54.6 mole % $CDCl_3/CCl_4$ (cm^{-1})	$CDCl_3$ (cm^{-1})
Pentane	86.43	86.55	86.99
Hexane	86.18	86.45	86.77
Heptane	86.05	86.37	86.75
Octane	85.80	86.13	86.53
Nonane	85.67	86.00	86.41
Decane	85.57	85.92	86.35
Undecane	85.44	85.80	86.28
Dodecane	85.37	85.76	86.27
Tridecane	85.29	85.71	86.19
Tetradecane	85.19	85.61	86.18
Octadecane	84.91	85.51	85.98

TABLE VI. Infrared data for $\nu_{asym}CH_2$ and $\nu_{sym}CH_2$ for *n*-alkanes in 0.5% solutions in CCl_4, 54.6 mole % $CDCl_3/CCl_4$, and $CDCl_3$.

	$\nu_{asym}CH_2$, $\nu_{sym}CH_2$		
Compound	CCl_4 (cm^{-1})	54.6 mole % $CDCl_3/CCl_4$ (cm^{-1})	$CDCl_3$ (cm^{-1})
Pentane	66.32	66.54	66.52
Hexane	66.60	68.84	69.11
Hexane	68.77	69.09	69.39
Heptane	69.48	69.89	70.21
Octane	70.40	70.77	71.04
Nonane	71.11	71.36	71.42
Decane	71.52	71.68	71.88
Undecane	71.67	71.86	71.98
Dodecane	71.80	71.96	72.13
Tridecane	71.87	72.01	72.19
Tetradecane	71.89	72.06	72.25
Octadecane	72.02	72.15	72.34
Δ cm^{-1}	5.70	5.61	5.82

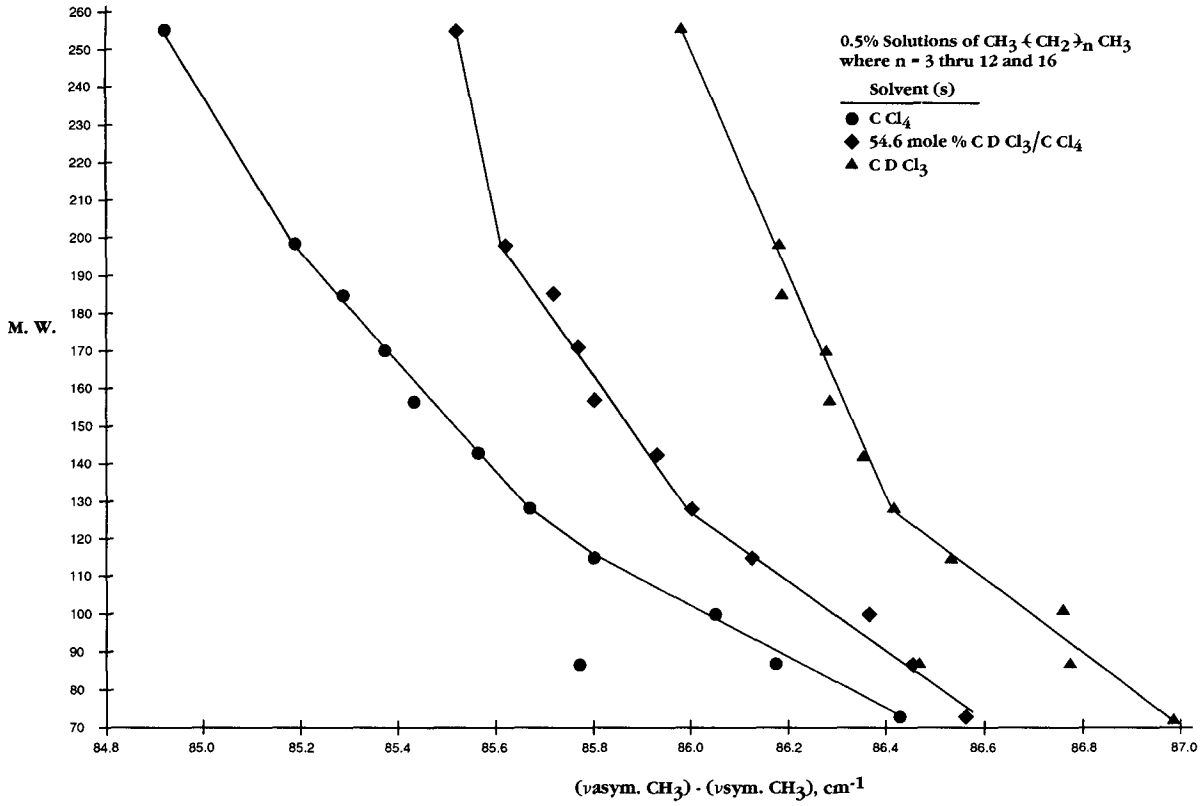

FIG. 8. Plots of the frequency separation ($\nu_{asym}CH_3 - \nu_{sym}CH_3$) vs. M.W. for each n-alkane in three different solvent systems.

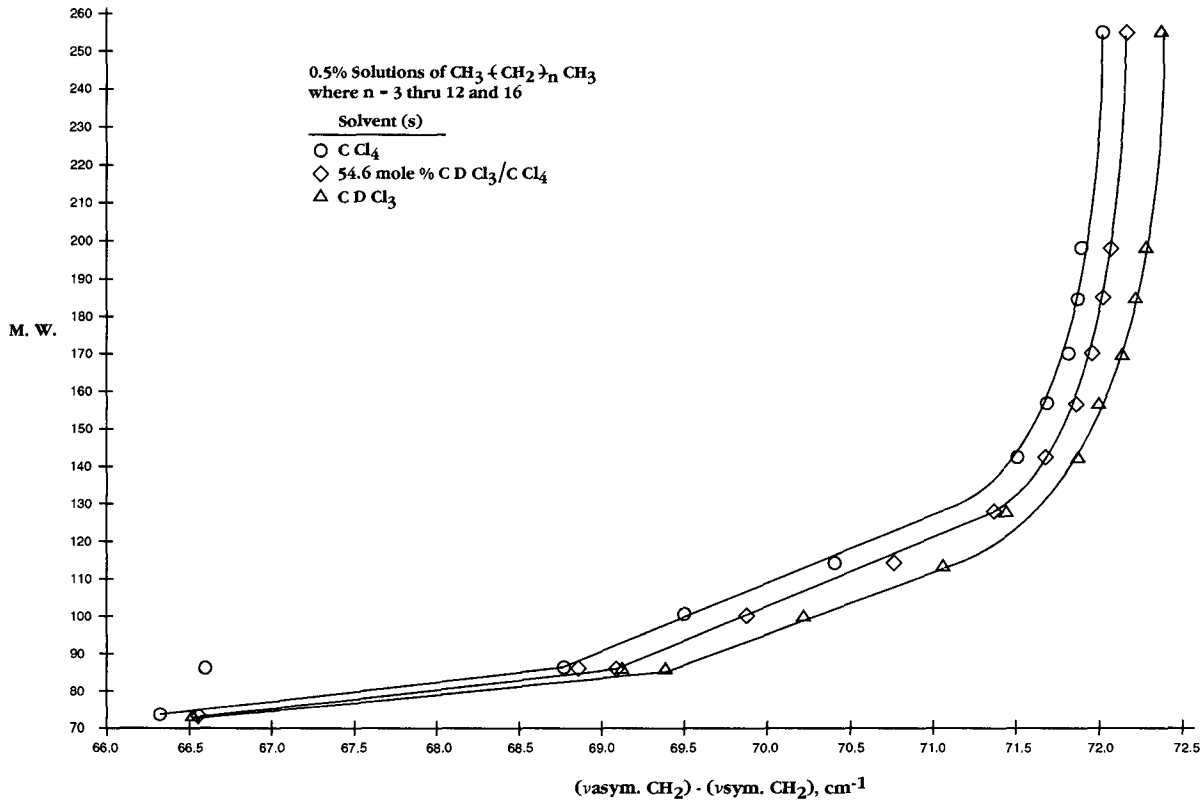

FIG. 9. Plots of the frequency separation ($\nu_{asym}CH_2 - \nu_{sym}CH_2$) vs. M.W. for each n-alkane in three different solvent systems.

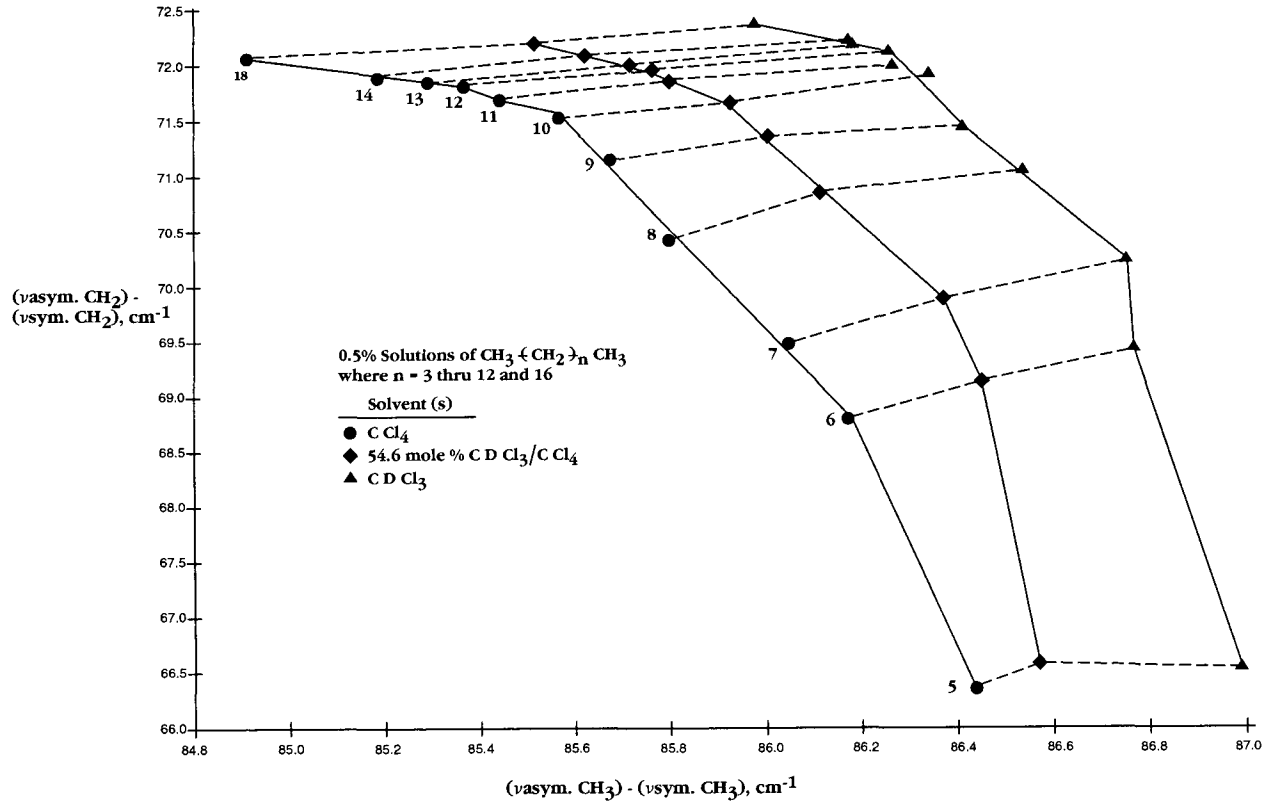

FIG. 10. Plots of the frequency separation ($\nu_{asym}CH_3 - \nu_{sym}CH_3$) vs. the frequency separation ($\nu_{asym}CH_2 - \nu_{sym}CH_2$) for each *n*-alkane in three different solvent systems.

of carbon atoms in *n*-alkanes increases there are more CH_2 groups stretching in phase in both the $\nu_{asym}CH_2$ and $\nu_{sym}CH_2$ vibrations. With the increasing number of CH_2 groups, both modes decrease in frequency; however, the $\nu_{sym}CH_2$ mode decreases more in frequency than the $\nu_{asym}CH_2$ mode, progressing in the series pentane through octadecane. Moreover, the rate of frequency decrease for $\nu_{sym}CH_2$ is larger than the rate of frequency decrease for $\nu_{asym}CH_2$ with the resultant increase in the frequency separation between $\nu_{asym}CH_2$ and $\nu_{sym}CH_2$ as the number of carbon atoms becomes larger in the *n*-alkane series.

Figure 10 shows plots of the frequency separation between ($\nu_{asym}CH_3$ and $\nu_{sym}CH_3$) vs. the frequency separation between ($\nu_{asym}CH_2$ and $\nu_{sym}CH_2$) for the *n*-alkanes in each of the solvent systems. Linear relationships are noted for heptane through octane and nearly linear relationships are noted between decane and octadecane. These plots clearly show that the frequency separation ($\nu_{asym}CH_3$–$\nu_{sym}CH_3$) decreases in frequency and the frequency separation ($\nu_{asym}CH_2$–$\nu_{sym}CH_2$) increases as the number of carbon atoms in the *n*-alkane increases.

Infrared Band Absorbance Ratios for νCH_3–νCH_2 and $\delta_{sym}CH_3$ Vibrations. The IR absorbance ratios reported in this section are the result of ratioing absorbance data (*A*) for $\nu_{asym}CH_3$, $\nu_{sym}CH_3$, $\nu_{asym}CH_2$, $\nu_{sym}CH_2$m, and $\delta_{sym}CH_3$ for the *n*-alkanes. The *A* values are measured peak heights for each of these four carbon-hydrogen stretching vibrations, and no correction has been made for band overlap.

Tables VII and VIII list absorbance data for νCH_3, δCH_3, and δCH_2 modes.

Table IX lists the absorbance ratios for $A(\nu_{asym}CH_3)/A(\nu_{sym}CH_3)$, $A(\nu_{sym}CH_2)/A(\nu_{asym}CH_2)$, $A(\nu_{asym}CH_3)/A(\nu_{sym}CH_2)$, and $A(\nu_{sym}CH_3)/A(\delta_{sym}CH_3)$.

Table X lists the absorbance ratios for $A(\nu_{asym}CH_3)/$

TABLE VII. Infrared absorbance data for *n*-alkanes in 0.5% solutions in CCl_4, 54.6 mole % $CDCl_3/CCl_4$, and $CDCl_3$.

Compound	$A(\nu_{asym}CH_3)$	$A(\nu_{asym}CH_2)$	$A(\nu_{sym}CH_3)$	$A(\nu_{sym}CH_2)$
Pentane	1.090	0.780	0.502	0.407
Hexane	0.879	0.759	0.408	0.402
Hexane	0.903	0.860	0.419	0.430
Heptane	0.769	0.925	0.372	0.450
Octane	0.670	0.938	0.329	0.458
Nonane	0.637	1.027	0.319	0.512
Decane	0.563	1.028	0.287	0.527
Undecane	0.538	1.083	0.283	0.558
Dodecane	0.478	1.073	0.256	0.560
Tridecane	0.496	1.197	0.271	0.632
Tetradecane	0.473	1.230	0.263	0.660
Octadecane	0.374	1.234	0.221	0.672

TABLE VIII. Infrared absorbance data for *n*-alkanes in 0.5% solutions in CCl_4, 54.6 mole % $CDCl_3/CCl_4$, and $CDCl_3$.

Compound	$A(\delta CH_2)$	$A(\delta_{asym}CH_2)$	$A(\delta_{sym}CH_3)$
Pentane	0.137	0.141	0.105
Hexane	0.127	0.115	0.082
Hexane	0.152	0.123	0.090
Heptane	0.147	0.111	0.084
Octane	0.128	0.096	0.073
Nonane	0.143	0.103	0.063
Decane	0.136	0.092	0.060
Undecane	0.134	0.093	0.057
Dodecane	0.132	0.084	0.050
Tridecane	0.141	0.081	0.051
Tetradecane	0.141	0.081	0.047
Octadecane	0.132	0.080	0.037

TABLE IX. Infrared absorbance data for *n*-alkanes in 0.5% solutions in CCl_4, 54.6 mole % $CDCl_3/CCl_4$, and $CDCl_3$.

Compound	$\frac{A(\nu_{asym}CH_3)}{A(\nu_{sym}CH_3)}$	$\frac{A(\nu_{sym}CH_2)}{A(\nu_{sym}CH_2)}$	$\frac{A(\nu_{asym}CH_3)}{A(\nu_{asym}CH_2)}$	$\frac{A(\nu_{sym}CH_3)}{A(\nu_{sym}CH_2)}$
Pentane	2.1710	1.916	1.397	1.233
Hexane	2.1540	1.912	1.143	1.015
Hexane	2.1553	2.000	1.050	0.974
Heptane	2.0670	2.064	0.831	0.827
Octane	2.0360	2.048	0.714	0.718
Nonane	1.9970	2.006	0.620	0.623
Decane	1.9620	1.951	0.548	0.545
Undecane	1.9010	1.941	0.497	0.507
Dodecane	1.8670	1.916	0.445	0.457
Tridecane	1.8300	1.894	0.414	0.428
Tetradecane	1.7980	1.864	0.385	0.398
Octadecane	1.6920	1.836	0.303	0.329

TABLE X. Infrared absorbance data for *n*-alkanes in 0.5% solutions in CCl_4, 54.6 mole % $CDCl_3/CCl_4$, and $CDCl_3$.

Compound	$\frac{A(\nu_{asym}CH_3)}{A(\nu_{sym}CH_2)}$	$\frac{A(\nu_{sym}CH_3)}{A(\nu_{asym}CH_2)}$	$\frac{A(\nu_{sym}CH_3)}{A(\delta_{sym}CH_2)}$
Pentane	2.678	0.644	4.781
Hexane	2.187	0.531	4.976
Hexane	2.100	0.500	4.656
Heptane	1.689	0.402	4.429
Octane	1.463	0.351	4.507
Nonane	1.244	0.311	5.063
Decane	1.068	0.279	4.783
Undecane	0.964	0.261	4.965
Dodecane	0.854	0.238	5.120
Tridecane	0.785	0.226	5.313
Tetradecane	0.717	0.214	5.596
Octadecane	0.557	0.179	5.972

$A(\nu_{sym}CH_2)$, $A(\nu_{sym}CH_2)/A(\nu_{asym}CH_2)$, and $A(\nu_{sym}CH_3)/A(\delta_{sym}CH_3)$.

Figure 11 shows a plot of $A(\nu_{asym}CH_3)/A(\nu_{sym}CH_2)$ vs. the M.W. of each *n*-alkane. This plot shows that the absorbance ratio *decreases* in a smooth manner as the M.W. or number CH_2 groups in the *n*-alkane increases.

Figure 12 shows a plot of $A(\nu_{sym}CH_3)/A(\nu_{sym}CH_2)$ vs. the M.W. of each *n*-alkane, and this plot is similar to the plot shown in Fig. 11.

Figure 13 shows a plot of $A(\nu_{asym}CH_3)/A(\nu_{asym}CH_2)$ vs. $A(\nu_{sym}CH_3)/A(\nu_{sym}CH_2)$ for *n*-alkanes, and Fig. 14 shows a plot of $A(\nu_{asym}CH_3)/A(\nu_{asym}CH_2)$ vs. $A(\nu_{sym}CH_3)/A(\nu_{sym}CH_2)$ for *n*-alkanes. Both plots show two linear segments—pentane through heptane, and heptane through octadecane. This result suggests that the effect of the CH_3 groups on these absorbance ratios is constant in the series heptane through octadecane.

δCH_2, $\delta_{asym}CH_3$, and $\delta_{sym}CH_3$ Vibrations. Table XI lists IR data for δCH_2, $\delta_{asym}CH_3$, and $\delta_{sym}CH_3$. These three modes are relatively unaffected by the number of carbon atoms in the *n*-alkane. The δCH_2 mode occurs in the region 1467.22–1467.63 cm^{-1}, the $\delta_{asym}CH_3$ mode occurs in the region 1457.97–1458.85 cm^{-1}, and the $\delta_{sym}CH_3$ mode occurs in the region 1378.39–1379.23 cm^{-1}.

SUMMARY

The *n*-alkanes are nonpolar molecules, and one would expect that there would be minimal solute–solvent interaction between *n*-alkanes and solvents such as CCl_4

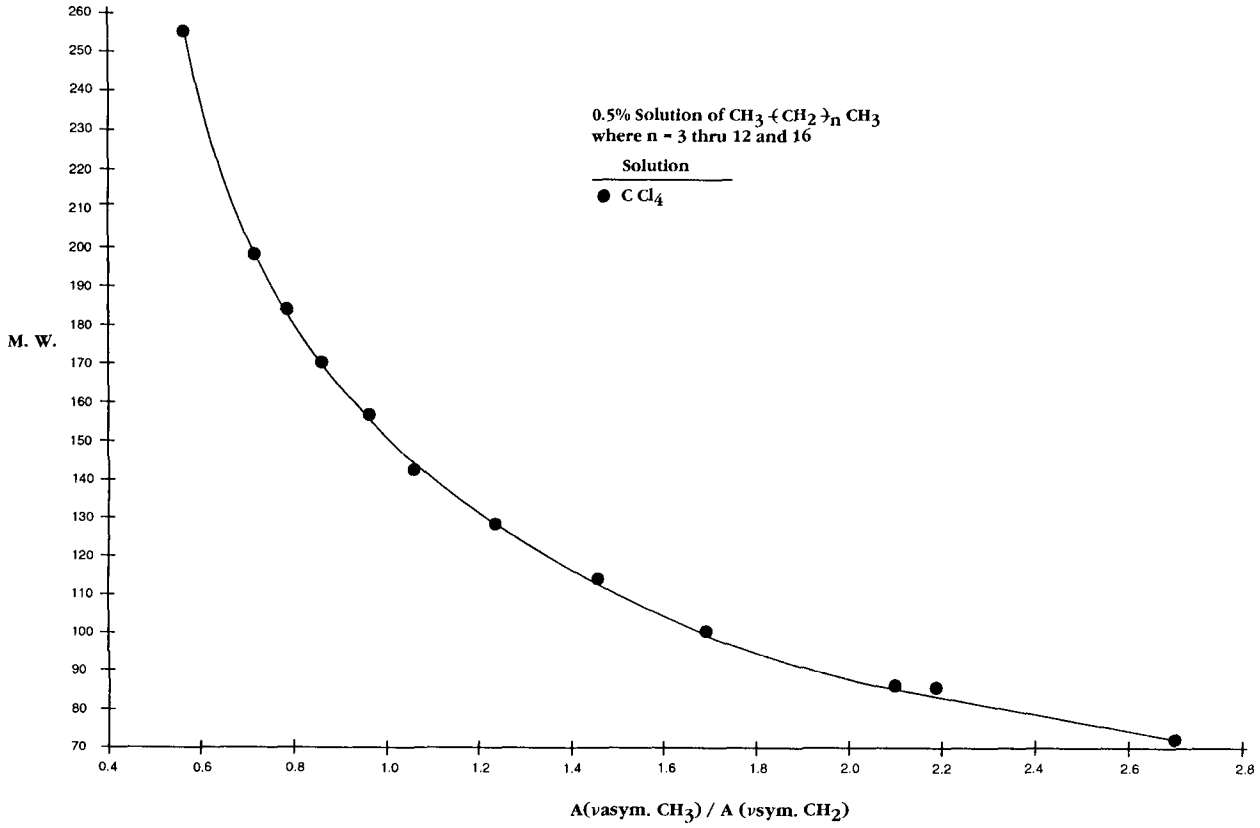

FIG. 11. A plot of $A(\nu_{asym}CH_3)/A(\nu_{sym}CH_2)$ vs. the M.W. of each *n*-alkane.

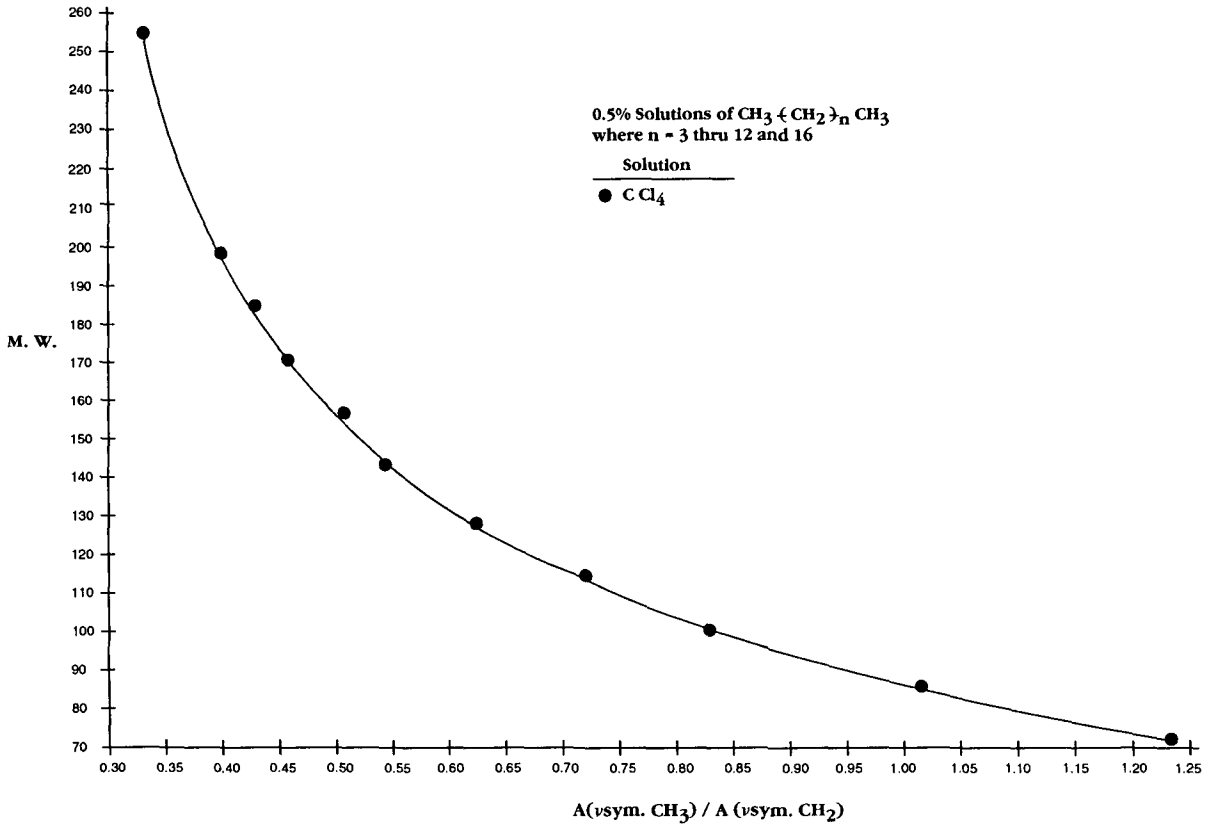

FIG. 12. A plot of the absorbance ratio $A(\nu_{sym}CH_3)/A(\nu_{sym}CH_2)$ vs. M.W. for each n-alkane in CCl_4 solution.

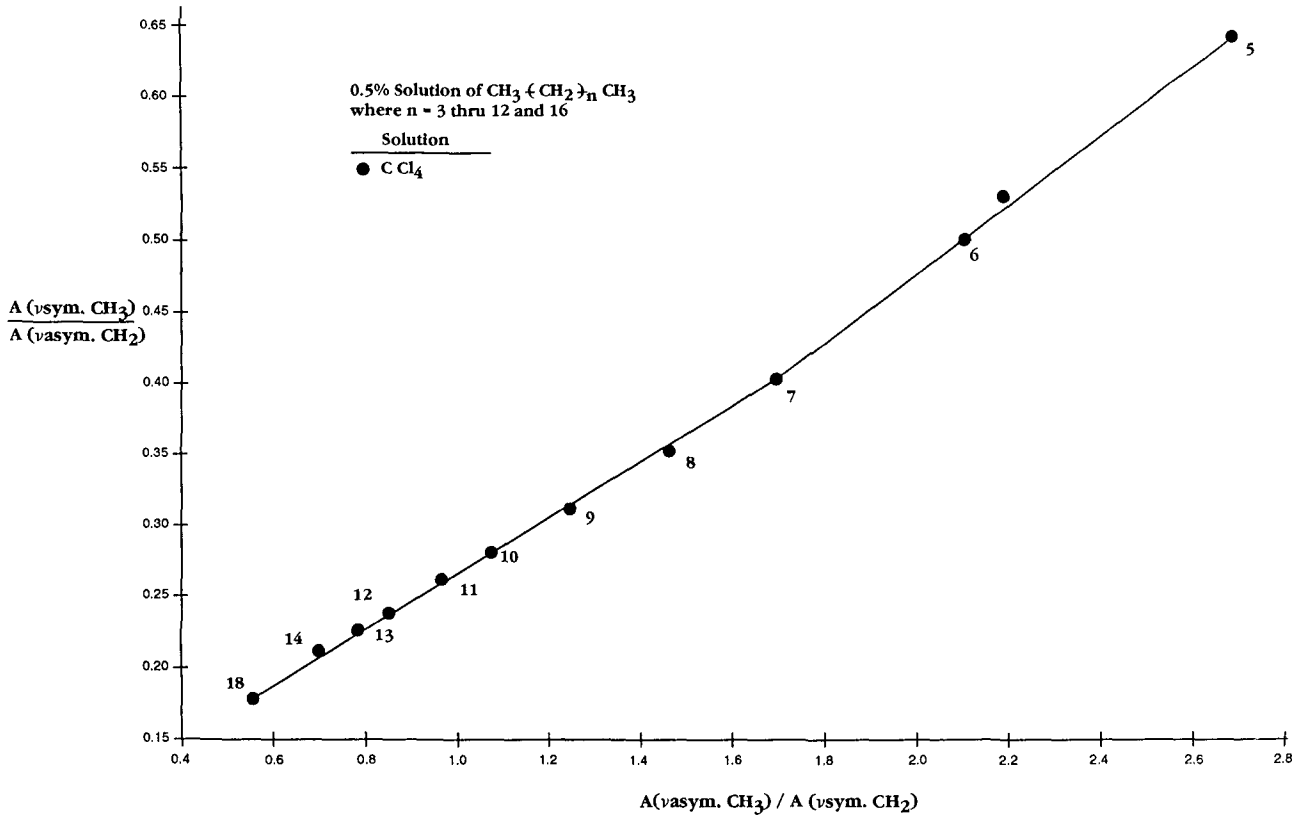

FIG. 13. A plot of the absorbance ratio $A(\nu_{asym}CH_3)/A(\nu_{asym}CH_2)$ vs. the absorbance ratio $A(\nu_{sym}CH_3)/A(\nu_{sym}CH_2)$ for n-alkanes in CCl_4 solution.

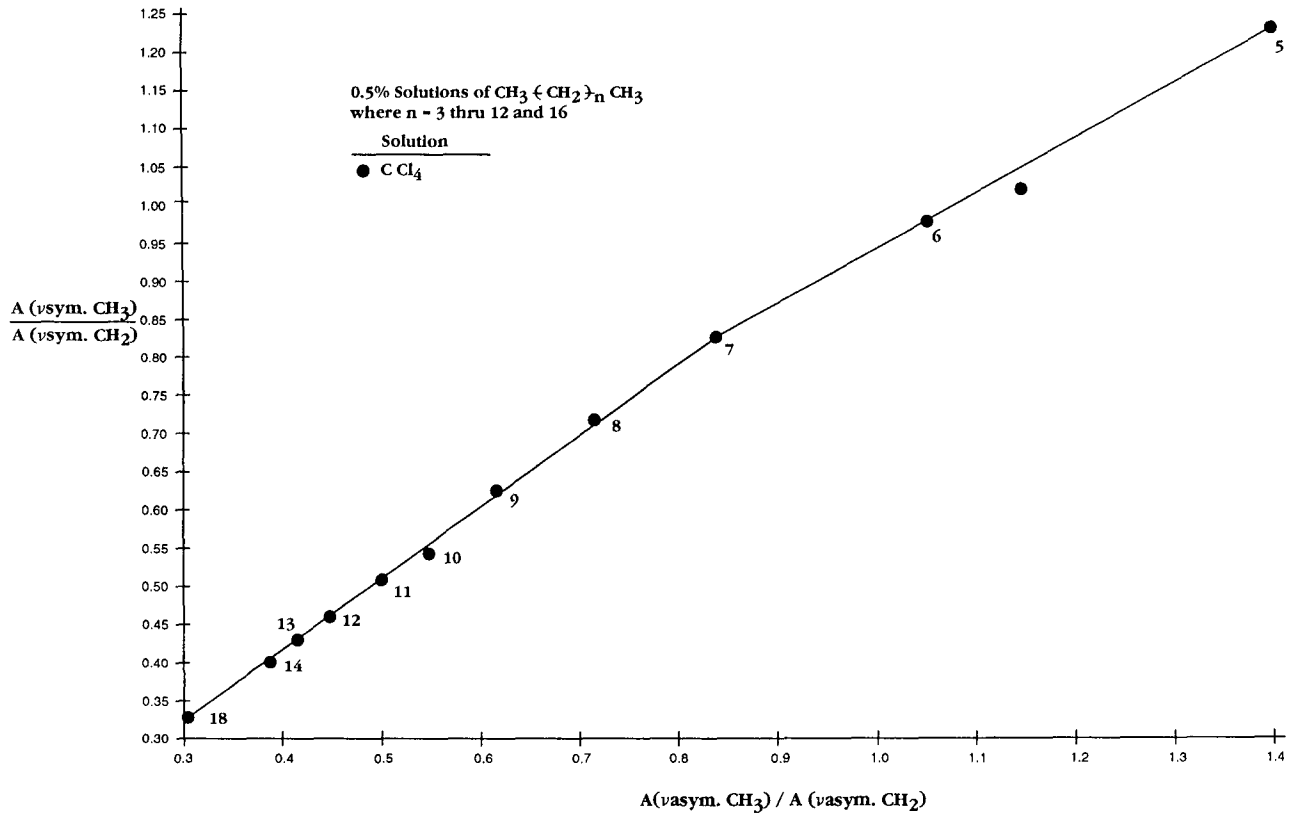

FIG. 14. A plot of the absorbance ratio $A(\nu_{asym}CH_3)/A(\nu_{sym}CH_2)$ vs. the absorbance ratio $A(\nu_{sym}CH_3)/A(\nu_{asym}CH_2)$ for n-alkanes in CCl_4 solution.

or $CDCl_3$. Our present study has shown that there is solvent interaction between n-alkane protons and CCl_4 and/or $CDCl_3$ Cl atoms, as noted by shifts in the molecular vibrations such as $\nu_{asym}CH_3$, $\nu_{sym}CH_3$, $\nu_{asym}CH_2$, and $\nu_{sym}CH_2$ where the $\nu_{asym}CH_3$ and $\nu_{asym}CH_2$ frequencies *increase* and the $\nu_{sym}CH_3$ and $\nu_{sym}CH_2$ frequencies *decrease* in going from dilute solution in CCl_4 to dilute solution in $CDCl_3$. The solute–solvent interactions causing shifts in these molecular vibrations are thought to be threefold. Physical restriction of the νCH_3 and νCH_2 proton vibrations due to the force of the solvent molecules exerted on the n-alkane in dilute solution has the effect of increasing the νCH_3 and νCH_2 frequencies. Another factor is the intermolecular hydrogen bonding between n-alkane protons and the free pair of electrons on the Cl atoms of either CCl_4 or $CDCl_3$. This factor is caused by the induced positive charge on n-alkane protons during the change in the dipole moment during the νCH_3 and νCH_2 vibrations. This effect causes the νCH_3 and νCH_2 modes to shift to lower frequency. The third is a solvent packing steric factor. In the case of $CDCl_3$ as the solvent, the deuteron of $CDCl_3$ repulses the CH protons of the n-alkanes during the νCH_3 and νCH_2 modes, and this behavior causes the Cl atoms of the $CDCl_3$ molecules to surround the protons of the n-alkanes, which exist in a planar zig-zag structure in an ordered intermolecularly hydrogen-bonded structure. This ordered structure allows the n-alkane protons to be nearer spatially to $CDCl_3$ Cl atoms and allows stronger intermolecular hydrogen bonds to be formed between the n-alkyl protons and the Cl atoms of $CDCl_3$ than is the case when n-alkanes are in CCl_4 solution, even though the Cl atoms of CCl_4 are more basic than the Cl atoms of $CDCl_3$. The strength of the intermolecular hydrogen bond between (C-H:Cl-C) components determines the degree of shift to lower frequency of νCH_3 and νCH_2.

The combination of these three factors is used to explain the frequency behavior of νCH_3 and νCH_2 in going from solution in CCl_4 to solution in $CDCl_3/CCl_4$ to solution in $CDCl_3$. This study also shows that the absorbance ratios of the νCH_3 and νCH_2 modes can be used in the elucidation of molecular structure. In addition this study has shown that $\nu_{asym}CH_3$, $\nu_{asym}CH_2$, $\nu_{sym}CH_3$, and $\nu_{sym}CH_2$ decrease in frequency in each of the solvent sys-

TABLE XI. Infrared data for δCH_2, $\delta_{asym}CH_3$, and $\delta_{sym}CH_3$ n-alkanes in 0.5% solutions in CCl_4.

Compound	δCH_2 (cm^{-1})	$\delta_{asym}CH_3$ (cm^{-1})	$\delta_{sym}CH_3$ (cm^{-1})	δCH_2 minus $\delta_{sym}CH_3$ (cm^{-1})	$\delta_{asym}CH_3$ minus $\delta_{sym}CH_3$ (cm^{-1})
Pentane	1467.55	1458.00	1379.23	88.32	78.77
Hexane	1467.22	1458.37	1378.48	88.74	79.89
Hexane	1467.35	1458.29	1378.59	88.76	79.70
Heptane	1467.39	1458.08	1378.66	88.73	79.42
Octane	1467.36	1458.85	1378.62	88.74	80.23
Nonane	1467.33	1458.27	1378.57	88.76	79.70
Decane	1467.39	1458.56	1378.39	89.00	80.17
Undecane	1467.63	1458.27	1378.60	88.76	79.67
Dodecane	1467.39	1458.27	1378.62	88.77	79.65
Tridecane	1467.36	1458.27	1378.64	88.72	79.63
Tetradecane	1467.35	1458.56	1378.61	88.74	79.95
Octadecane	1467.33	1457.97	1378.64	88.69	79.33

tems studied as n for CH_3-$(CH_2)_n$-CH_3 increases. No previous study of alkanes has shown this trend.

1. D. Lin-Vien, N. B. Colthup, W. G. Fateley, and J. G. Grasselli, *The Handbook of Infrared and Raman Characteristic Frequencies of Organic Molecules* (Academic Press, San Diego, 1991).
2. N. B. Colthup, L. H. Daly, and S. E. Weberley, *Introduction to Infrared and Raman Spectroscopy* (Academic Press, San Diego, 1990).
3. R. A. Nyquist, Appl. Spectrosc. **40,** 79 (1986).
4. R. A. Nyquist, Appl. Spectrosc. **40,** 336 (1986).
5. R. A. Nyquist, V. Chrzan, and J. Houck, Appl. Spectrosc. **43,** 981 (1989).
6. R. A. Nyquist, C. L. Putzig, and L. Yurga, Appl. Spectrosc. **43,** 1049 (1989).
7. R. A. Nyquist, T. M. Kirchner, and H. A. Fouchea, Appl. Spectrosc. **43,** 1053 (1989).
8. R. A. Nyquist, Appl. Spectrosc. **43,** 1208 (1989).
9. R. A. Nyquist, Appl. Spectrosc. **43,** 1374 (1989).
10. R. A. Nyquist, V. Chrzan, T. M. Kirchner, L. Yurga, and C. L. Putzig, Appl. Spectrosc. **44,** 243 (1990).
11. R. A. Nyquist, Appl. Spectrosc. **44,** 425 (1990).
12. R. A. Nyquist, Appl. Spectrosc. **44,** 433 (1990).
13. R. A. Nyquist, Appl. Spectrosc. **44,** 438 (1990).
14. R. A. Nyquist, Appl. Spectrosc. **44,** 783 (1990).
15. R. A. Nyquist and S. E. Settineri, Appl. Spectrosc. **44,** 791 (1990).
16. R. A. Nyquist, Appl. Spectrosc. **44,** 1405 (1990).
17. R. A. Nyquist and S. E. Settineri, Appl. Spectrosc. **44,** 1552 (1990).
18. R. A. Nyquist and S. E. Settineri, Appl. Spectrosc. **44,** 1629 (1990).
19. R. A. Nyquist and S. E. Settineri, Appl. Spectrosc. **45,** 92 (1991).
20. R. A. Nyquist, H. A. Foucher, G. A. Hoffman, and D. L. Hasha, Appl. Spectrosc. **45,** 860 (1991).
21. R. A. Nyquist and S. E. Settineri, Appl. Spectrosc. **45,** 1075 (1991).
22. R. A. Nyquist, D. A. Luoma, and D. W. Wilkening, Vib. Spectrosc. **2,** 61 (1991).
23. R. A. Nyquist and D. A. Luoma, Appl. Spectrosc. **45,** 1491 (1991).
24. R. A. Nyquist and D. A. Luoma, Appl. Spectrosc. **45,** 1497 (1991).
25. R. A. Nyquist, Appl. Spectrosc. **46,** 306 (1992).
26. R. A. Nyquist, S. E. Settineri, and D. A. Luoma, Appl. Spectrosc. **46,** 293 (1992).
27. R. A. Nyquist and C. L. Putzig, Vib. Spectrosc. **3,** 35 (1992).
28. R. A. Nyquist and G. L. Jewett, Appl. Spectrosc. **46,** 181 (1992).
29. R. A. Nyquist, D. A. Luoma, and C. L. Putzig, Appl. Spectrosc. **46,** 972 (1992).
30. R. A. Nyquist, D. A. Luoma, and C. W. Puehl, Appl. Spectrosc. **46,** 1273 (1992).
31. R. A. Nyquist and C. W. Puehl, Appl. Spectrosc. **46,** 1552 (1992).
32. R. A. Nyquist and C. W. Puehl, Appl. Spectrosc. **46,** 1564 (1992).
33. R. A. Nyquist, C. W. Puehl, and C. L. Putzig, Vib. Spectrosc. **4,** 193 (1992).
34. R. A. Nyquist and C. W. Puehl, Appl. Spectrosc. **47,** 677 (1993).
35. R. A. Nyquist, D. A. Luoma, and C. W. Puehl, Appl. Spectrosc. **47,** in press (1993).
36. R. A. Nyquist, Appl. Spectrosc. **47,** 450 (1993).